DOE/SF/21271-2

EARLY-TIME MEASUREMENTS OF LASER-PLASMA CONDITIONS IN OMEGA-UPGRADE ICF TARGETS

Final Report
April 1, 1997 - March 31, 1998

Hans R. Griem and Raymond C. Elton
University of Maryland
College Park, MD 20742-3511

DISCLAIMER

April 4, 1998

Prepared for the U.S. Department of Energy
Under Grant Number DE-FG03-97SF21271

Final Report

EARLY-TIME MEASUREMENTS OF LASER-PLASMA CONDITIONS IN OMEGA-UPGRADE ICF TARGETS

Under this FY-97 NLUF grant, we primarily carried out spectral line and continuum diagnostics at early times and in the coronal region of the plasma using our flat-field grazing-incidence spectrograph, improved to incorporate time resolution at wavelengths extending below the carbon K-absorption edge using a gated microchannel plate detector. These experiments were carried out on the OMEGA facility at the University of Rochester Laboratory for Laser Energetics (LLE). The experimental layout is shown in Fig. 1. Fifty-nine beams (one beam was reserved for scattering diagnostics) were focused onto the target, providing nominally 18 kJ of energy in a 1 ns pulse for an irradiance of ~2×10^{14} W/cm^2. Some beam smoothing, provided by spectral dispersion (SSD), was used, but may not have been particularly effective alone, i.e., without the presence of distributed phase plates (DPP's) in the beams. The plastic microballoon targets were nominally 900 μm in diameter with 10- and 20-μm thick walls, and were filled with neon to a pressure of 10 atm. Overcoatings of Mg and Al in thicknesses ranging from 0.2 to 4 μm were applied. A 1-μm thick layer of CH was added in some early shots to reduce the rate of expansion of the matallic coatings. For targets with primarily a magnesium coating, a 0.03-μm (300-Å) thick aluminum under-layer was applied over the plastic microballoon to seal-in the neon. In all, we obtained 44 data shots in 7.5 days spread over two weeks in June and September of 1997.

Our latest results were presented at the 1997 American Physical Society Division of Plasma Physics Conference in Pittsburgh in November 1997. A copy of the abstract is attached. In the extreme ultraviolet (euv) spectral region, we observed n=3 to n=2 emissions from Li-, He- and H-like ions from the Mg and Al coatings. We also obtained evidence confirming our previously-published [1] (time-integrated) laser-field-induced satellites lines at 53.1 Å and 62.8 Å, apparently at the peak of the Gaussian drive pulse. Both the Mg-line and the continuum euv emissions are high during the radial collapse. The metallic coating materials appear to be in place to some degree during the compression phase, i.e., are not all blown away as coronal plasma at earlier times as modeled. This also is apparent in the Al Lyman-α x-ray measurements before and after compression. Here, however, higher line opacity made it difficult to track the resonance

lines through the compression phase. This illustrates the importance of euv measurements of less opaque lines at high densities.

The metallic euv spectral lines appear to be unusually short, which is an indication of some spatial resolution. This suggests that at least some of the Mg (and Al) is compressed at the peak of the Gaussian drive pulse and before collapse, i.e., does not simply expand away. (This observation is supported by streak x-ray data described below.) The euv results are shown in Figs. 2-5. In Fig. 2b it is indicated that a rather strong Li-like Mg X 2p-3d "resonance" line at 63 Å begins to emit at t=0 (defined somewhat arbitrarily). Previous to this zero point by -1 ns were seen lower ionization stages such as Mg V and O V, VI lines in the 150-Å range (Fig. 2a), arriving very early. The observation of these early ionic species is a major emphasis in our work. This was accomplished here with more magnesium present in thicker layers and will continue to improve with our new TIM-mounted spectrograph (described in the next section and shown in a photo in Fig. 10) closer to the plasma. At t=+1 ns on this scale, the Mg X line disappears (see Fig. 3a), as presumably most of the Mg coating is blown away (all of it according to the model) or perhaps completely stripped. (This is consistent with the x-ray streak data shown later in Fig. 6 on a corresponding time scale.) By t=2 ns (Fig. 3b), the continuum has reached a D=2 density level as the inner CH microballoon begins to collapse and Mg X, XI and XII (hydrogenic) lines reappear, along with the cold carbon continuum absorption at the 44 Å K-edge (designated C-K in some of the figures). Clearly not all of the magnesium has expanded away, or it would not be reobserved during compression. This data again agrees with the timing of the x-ray spectral continuum (Fig. 6). At t=3 ns, the euv continuum peaks (Fig. 4a), and begins to decline by t=5 ns (Fig. 4b). This euv continuum is much more sustained in time than the x-ray continuum, which occurs in a higher-energy and hotter plasma of shorter duration. By t=7 ns, the spectrum appears to be dominated by recombination into Mg and C ions, as shown in Fig. 5.

Late-time (after compression) euv spectral emission from Li-like neon from the core filling gas was observed in 1997 with thinner-shell targets only. It may be that the thicker CH wall traps the neon line emission. An estimate of continuum absorption at a wavelength of 98 Å (Ne VIII 2p-3d transition line) by inverse bremsstrahlung [2] gives a calculated absorption coefficient of 0.9/mm or an opacity approximately equal to 18 for a 20-μm thick layer. In future experiments we hope to include argon in the gas fill as a minority admixture with neon, and observe second-order x-ray resonance lines

simultaneously with first-order Mg lines (as we have done with chlorine in the past, described next). Whether these high-temperature lines continue to exist after SSD-with-DPP beam smoothing is included is an interesting question to be answered in future experiments.

A corresponding (in time) x-ray spectrum obtained with an LLE/LLNL streak crystal spectrograph is shown in Fig. 6, as already mentioned. Besides the Mg and Al (sealant) lines, some Lyman-α and -β lines from Cl XVII (impurity) are present (in second order) near the peak of the drive pulse and at a wavelength of ~ 3.5-4 Å ($h\nu$ =3-3.5 keV), where the beryllium filter transmits well. This implies a temperature reaching the keV range. From the x-ray spectral data (as suggested by the euv data described above), a continuum hump at the time of the Gaussian laser peak can be associated with magnesium, from evidence of a helium-like Mg XI recombination edge. Also evident in the x-ray data are two superimposed spatial components of the Al XIII Lyman-α line time history--one spreading (in the wavelength direction) with layer expansion and the other compressing. Such a spatial effect is observable from the spectral data because of the slitless nature of the x-ray crystal streak spectrograph, so that the spectral line width is determined by the source size. This dual-plasma effect is not included in the modeling at present, so that this observation could be a benchmark experimental point in code validation and useful in capsule instability/mix experiments. For example, it may be that the magnesium is becoming imbedded in hot spots formed in the target surface and hence carried into the collapse phase.

With thicker coatings, we were able to identify "j" and "k" Li-like x-ray satellites to the He-like Al XII $1s^2\ ^1S$-$1s2p\ ^1P$ resonance line at 7.878 Å and 7.875 Å, respectively. The relative intensities of these satellites can provide a value for the electron temperature either analytically or with more detailed numerical modeling. Likewise, it was observed that the Al XII $1s^2\ ^1S$-$1s2p\ ^3P$ intercombination line is unobservable, indicating collisional mixing and depopulation at electron densities $>10^{21}$ cm^{-3}.

We have been fortunate to obtain supporting modeling from Drs. J. Delettrez and R. Epstein of LLE for the particular shot discussed above. The results for the hydrodynamic modeling of the expansion of the initially 2000-Å thick Mg (and 300-Å thick Al) coatings and the collapse of the shell with increasing electron density are shown in Fig. 7a. In this figure, time is measured from the beginning of the nominally 1-ns Gaussian pulse, which is approximated by a triangular pulse beginning at the origin,

peaking at 1 ns, and returning to zero at 2 ns. Corresponding computations of electron density N_e and temperature T_e are shown in Fig. 7b. Collapse occurs between 2.5 and 3 ns, which agrees with Figs. 2-6 if t=0 is defined at the start of the pulse. Computed spectra for the n=2 to n=1 transitions in He- and H-like Mg XI and XII and Al XII and XIII, respectively, are plotted on the same time scale in Fig. 8. Shown here is the sequence of initially burning through He-like to H-like Mg from the outer layer as the temperature rises, followed by He-like and then H-like Al from the sealant layer beneath, as observed experimentally. The very early peak in Mg line emission may be an artifact of the triangular pulse shape assumed, since a slower rise was indicated in the measured spectrum as well as in earlier modeling of another case (with a CH overcoating) for a pure Gaussian pulse shown in Fig. 9 and described in the next paragraph. This is currently being verified. One may note also in Fig. 8 the prediction of enhanced emission from these species following the collapse, as observed spectroscopically. This is most likely from recombination during the expansion period indicated in Fig. 7, and not necessarily associated with compression as indicated by the narrowing of x-ray lines whose widths depend on the source size (discussed above).

In Fig. 9(b) are shown first some LLE spectral modeling of n=2 to n=1 x-ray lines for an earlier target design consisting of 2000 Å of Mg over 2000 Å of Al adjacent to the CH microballoon, and a 1-μm thick CH overcoating. Accompanying this in Fig. 9(a) is a Gaussian pulse on the same time scale. Partial results from some preliminary 1-D LASNEX calculations for this case by Dr. J. Moreno of LLNL for n=3 to n=2 transitions radiating in the euv region are included for comparison in Fig. 9(b), where the time scale has been adjusted to show the similarity. This data is scaled down in intensity so as not to overlap the results of the LLE x-ray modeling.

The construction of our new TIM-mounted euv flat-field spectrograph (following an earlier design in Ref. 3) covering the spectral range of 30-250 Å (hν=50-400 eV), intended for initial use on OMEGA in FY-98, is well underway and will allow enhanced sensitivity by more than an order of magnitude as the distance from the slit to the target is shortened. A photograph of the new instrument in the open mode is shown in Fig. 10. In January 1998 a prototype was successfully test-fitted at LLE into a TIM. In March 1998 the light-tight enclosure was complete, and photographic spectra were successfully obtained using our ruby-laser beam focused onto a boron carbide target. The spectral range covered is 33-300 Angstroms. It will be fielded at LLE during our

first FY-98 series of shots presently scheduled for May 4-8, 1998, together with our earlier externally-mounted spectrograph incorporating time-resolved MCP detection.

REFERENCES

1. R.C. Elton, H.R. Griem, B.L. Welch, A.L. Osterheld, R.C. Mancini, J. Knauer, G. Pien, R.G. Watt, J.A. Cobble, P.A. Jaanimagi, D.K. Bradley, J.A. Delettrez and R. Epstein, J. Quant. Spectrosc. Radiat. Transfer **58**, 559 (1997).

2. Naval Research Laboratory "Plasma Formulary", 1994, page 57; from T.W. Johnston and J.M. Dawson, Phys. Fluids **16**, 722 (1973).

3. T. Harada and T. Kita, Appl. Optics **19**, 3987 (1980); T. Kita, T. Harada, N. Nakano and H . Kuroda, Appl. Optics **22**, 512 (1983); and N. Nakano, H. Kuroda, T. Kita and T. Harada, Appl. Optics **23**, 2386 (1984).

39th Annual Meeting, APS Division of Plasma Physics
17-21 November 1997, Pittsburgh, PA
Abstract Submittal Form
Deadline: Wednesday, 8 July 1997

⊗

Subject Classification Category: 4.8/E **Experiment**
(Laser-produced plasmas/diagnostics)

Time-Resolved X-ray Spectroscopy on OMEGA* R. ELTON, E. IGLESIAS, H. GRIEM, S. GOLDSMITH†, University of Maryland Institute for Plasma Research, and J. DELETTREZ, R. EPSTEIN, G. PIEN, D. BRADLEY, University of Rochester Laboratory for Laser Energetics--Soft x-ray spectroscopic diagnostics have been fielded on a plasma generated using 59 beams of the OMEGA laser at LLE, operated at 20 kJ total energy and 1-ns duration. The beams were focused onto neon-filled (10 Atm) microballoon targets of 900-μm diameter, coated with alternating layers of Mg and Al and overcoated with a 1-μm layer of CH. The irradiance varied from (1-4)10^{14} W/cm^2. Instrumentation included a 1-m flat-field soft x-ray spectrograph with a time-gated microchannel plate detector, a crystal spectrograph with streak camera/CCD detection, and a multi-frame time-gated x-ray pinhole camera. Of specific interest were certain xuv spectral lines and profiles from $n \geq 3$ to n=2 transitions in 1-,2- and 3-electron ions of coatings and fill gas, as well as laser-field induced satellites to forbidden transitions. The temporal history of x-ray resonance lines are compared with numerical modeling. Continuum steps at the series limit are used to derive an electron density for comparison with other techniques.

*Work supported by DoE. †Perm. Address: Tel Aviv University.

⊗

Prefer Poster Session

Submitted by:

_____
(Signature of APS Member)

Raymond C. Elton
(Member Name Typewritten)
Institute for Plasma Physics
University of Maryland
Ph. (301) 405-4995; FAX (301) 314-9437
elton@plasma.umd.edu

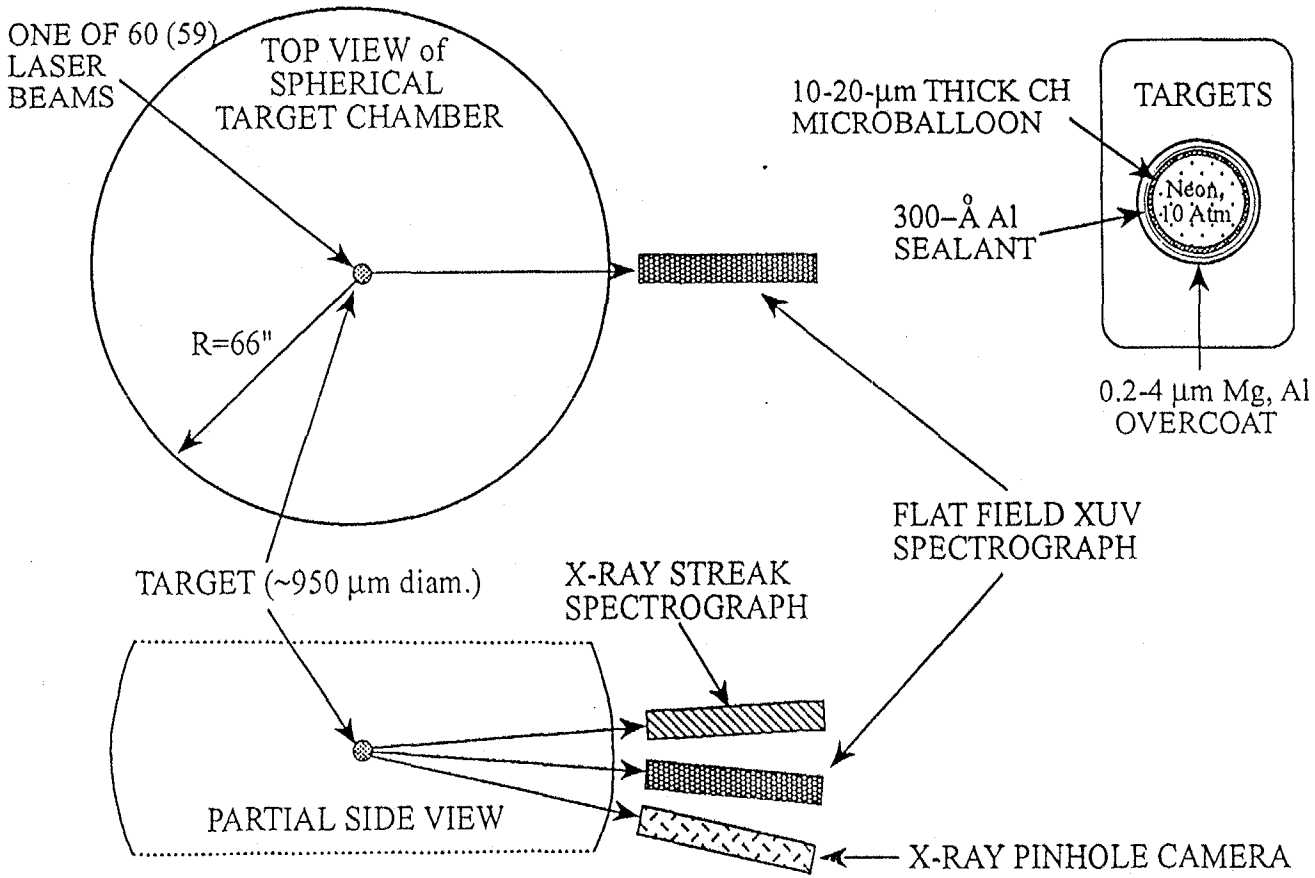

Fig. 1. Layout for 1997 experiments

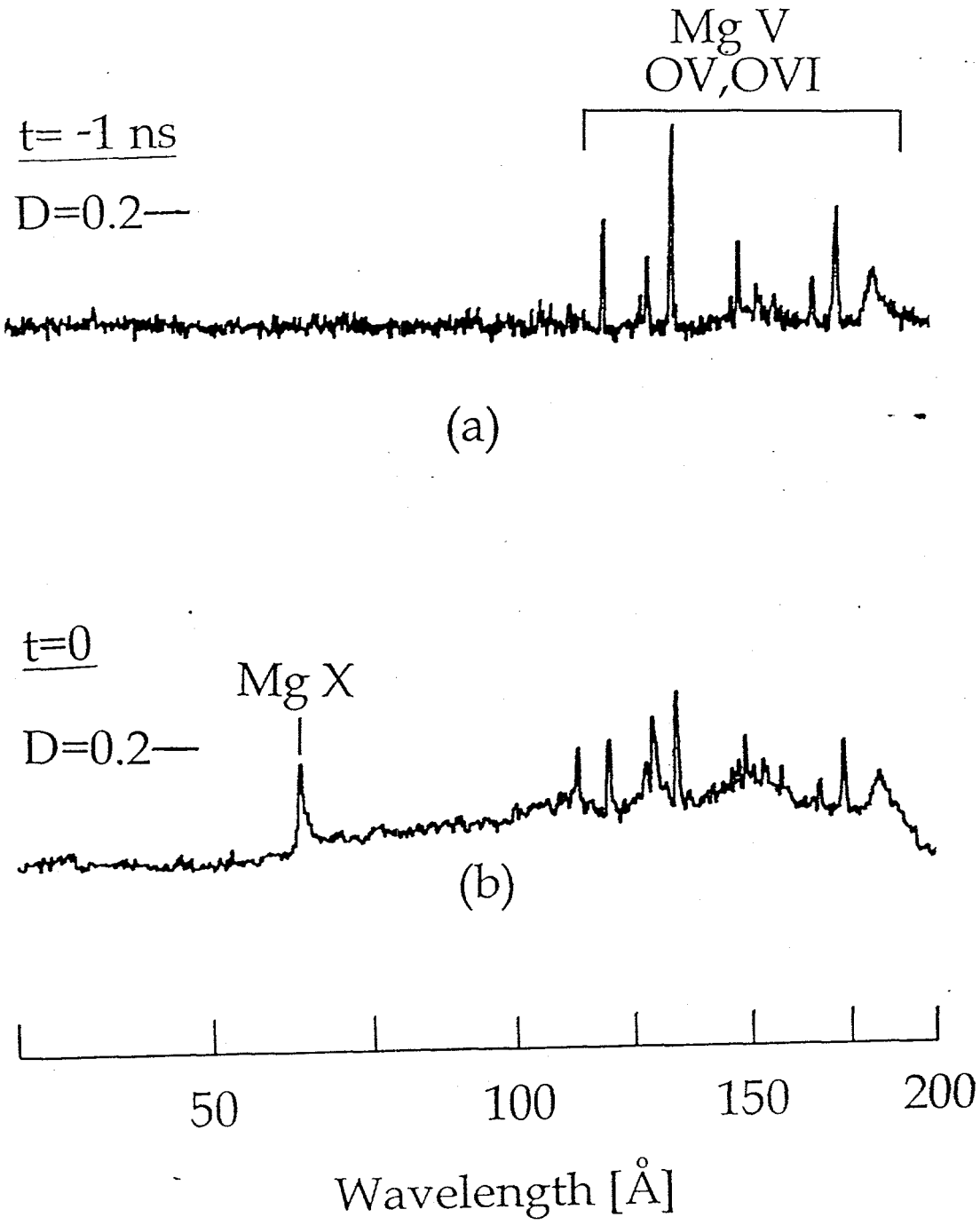

Fig. 2. Gated euv spectra at early times. The start at t=0 is set arbitrarily here (b) when the first highly ionized (Mg X) line appears. Photographic density is indicated by "D=" for comparison purposes.

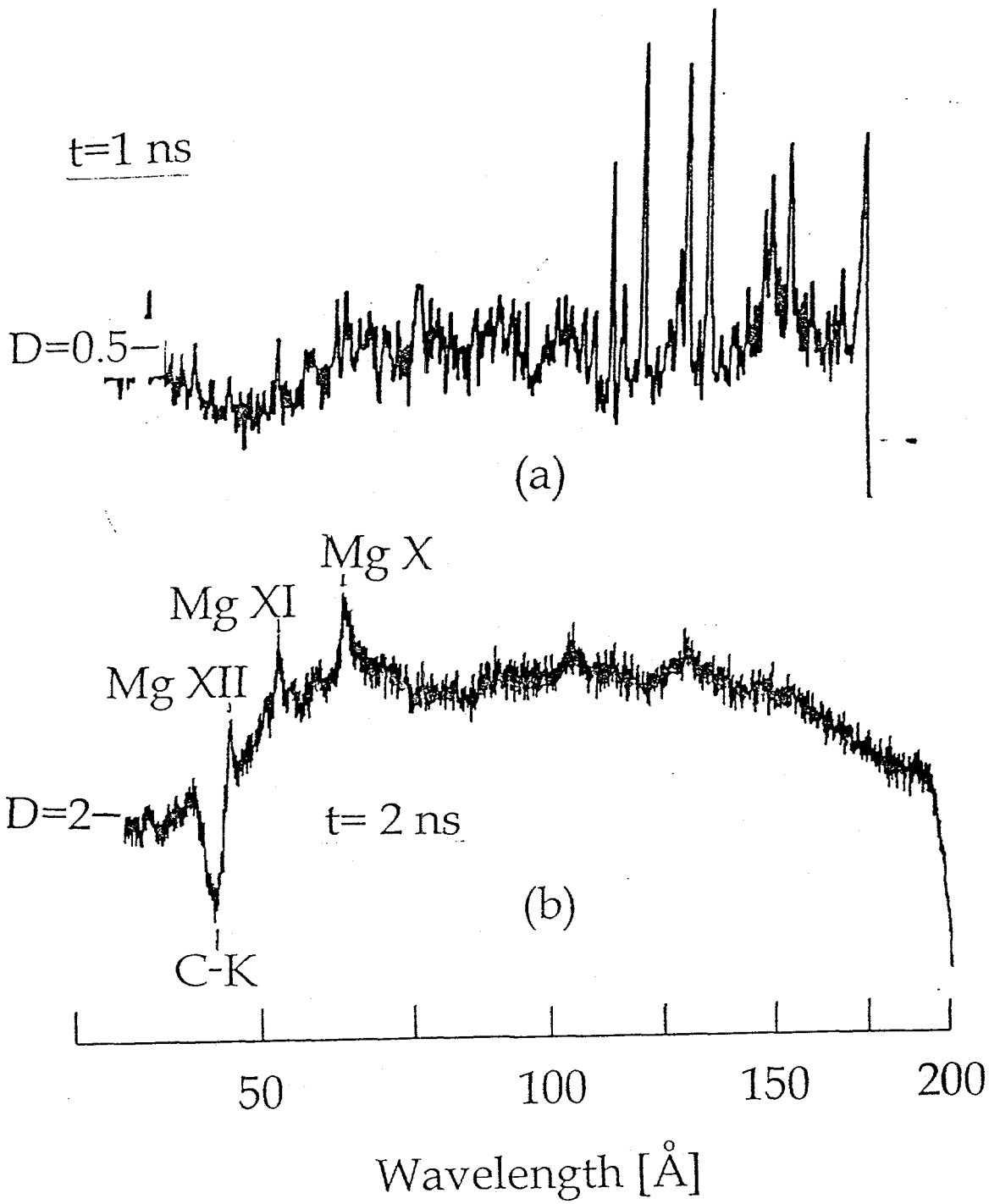

Fig. 3. Gated euv spectra showing the absence (a) of highly ionized Mg after the intial blowoff and ionization of much of the coating, and the return (b), along with cold-carbon absorption ("C-K"), as collapse begins.

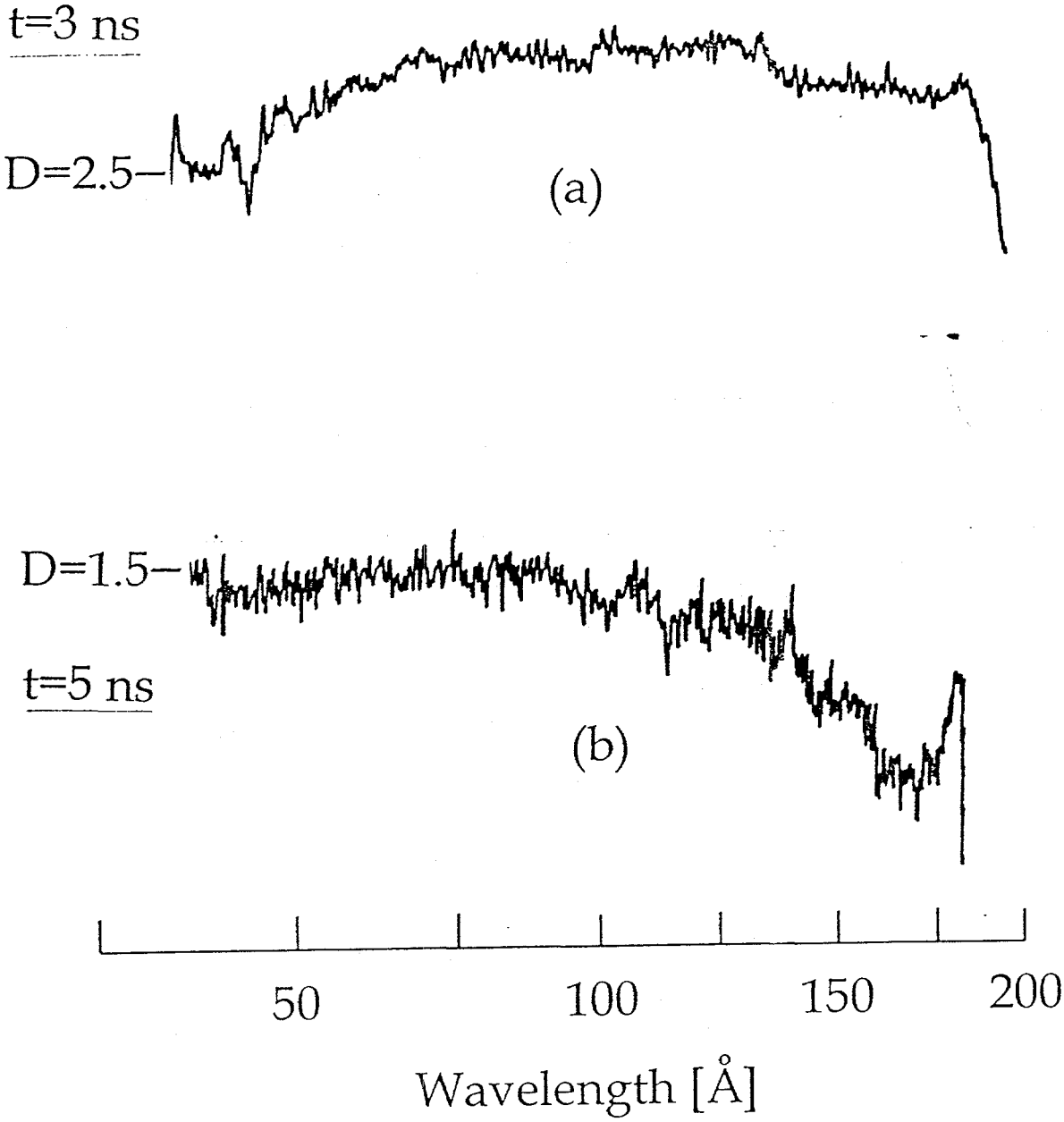

Fig. 4. Gated euv spectra during an extended (compared to x-ray data) collapse phase, where the photographic density "D=" is high.

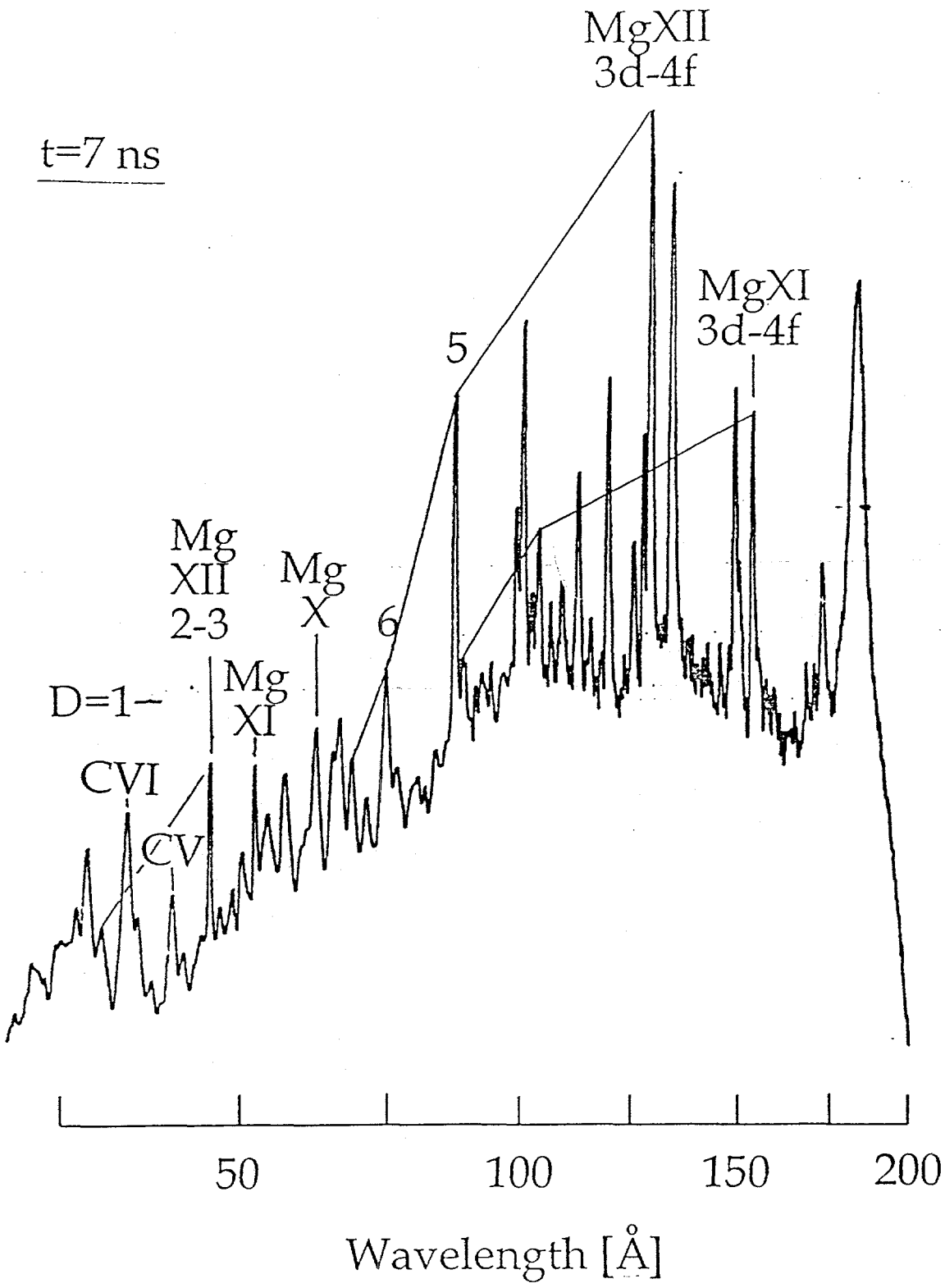

Fig. 5. Gated euv spectra following the collapse phase, showing recombination features such as high n,l lines of Mg XI and XII

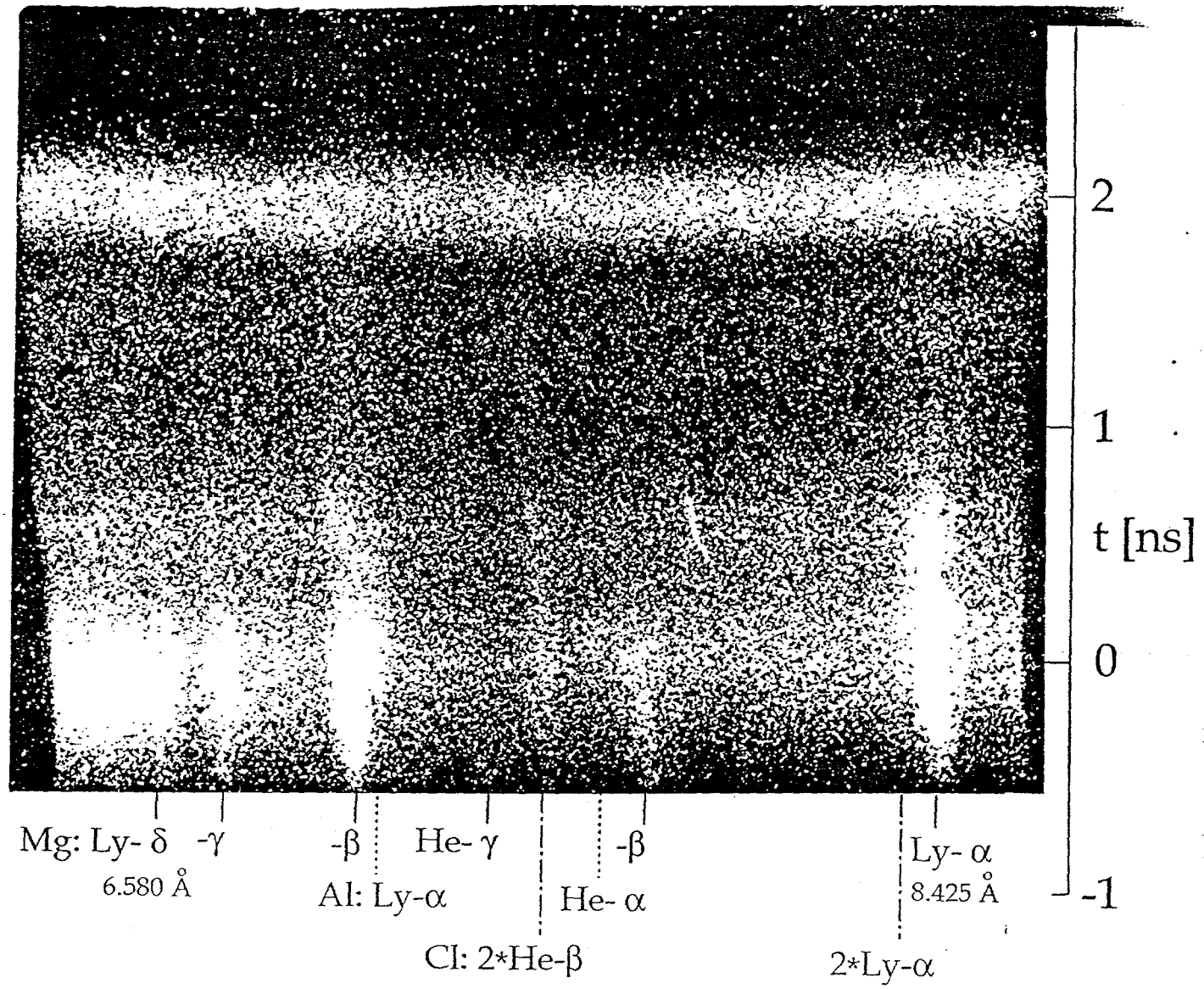

Fig. 6. Streak x-ray data showing resonance lines of Mg, as well as Al from the thin (300 Å) sealant layer. Time resolved features can be compared to the gated euv data. Longer wavelength lines are suppressed by the beryllium debris shields/filters present. Second order lines from Cl (impurity) are also indicated.

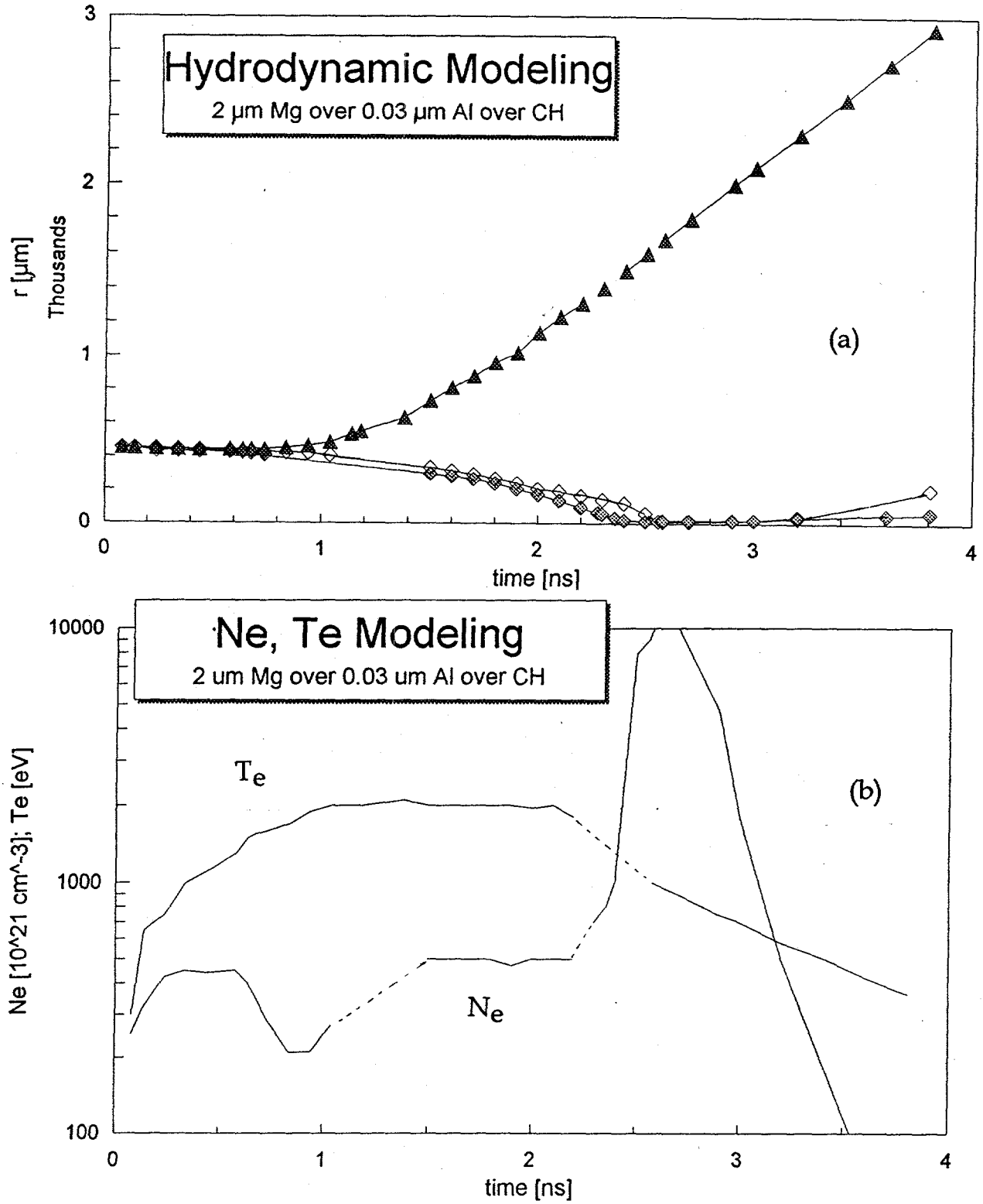

Fig. 7. Hydrodynamic modeling (a) of the expanding (radially up to 3 mm) 2000-Å thick Mg (and 300-Å thick Al) coatings (closed triangles), the collapsing shell (closed diamonds), and the closely-following peak electron density (open diamonds), for a 0-2 ns "Gaussian" drive pulse peaking at 1 ns. Shown in (b) versus time is the peak electron density in units of 10^{21} cm^{-3} and the peak coronal temperature in eV.

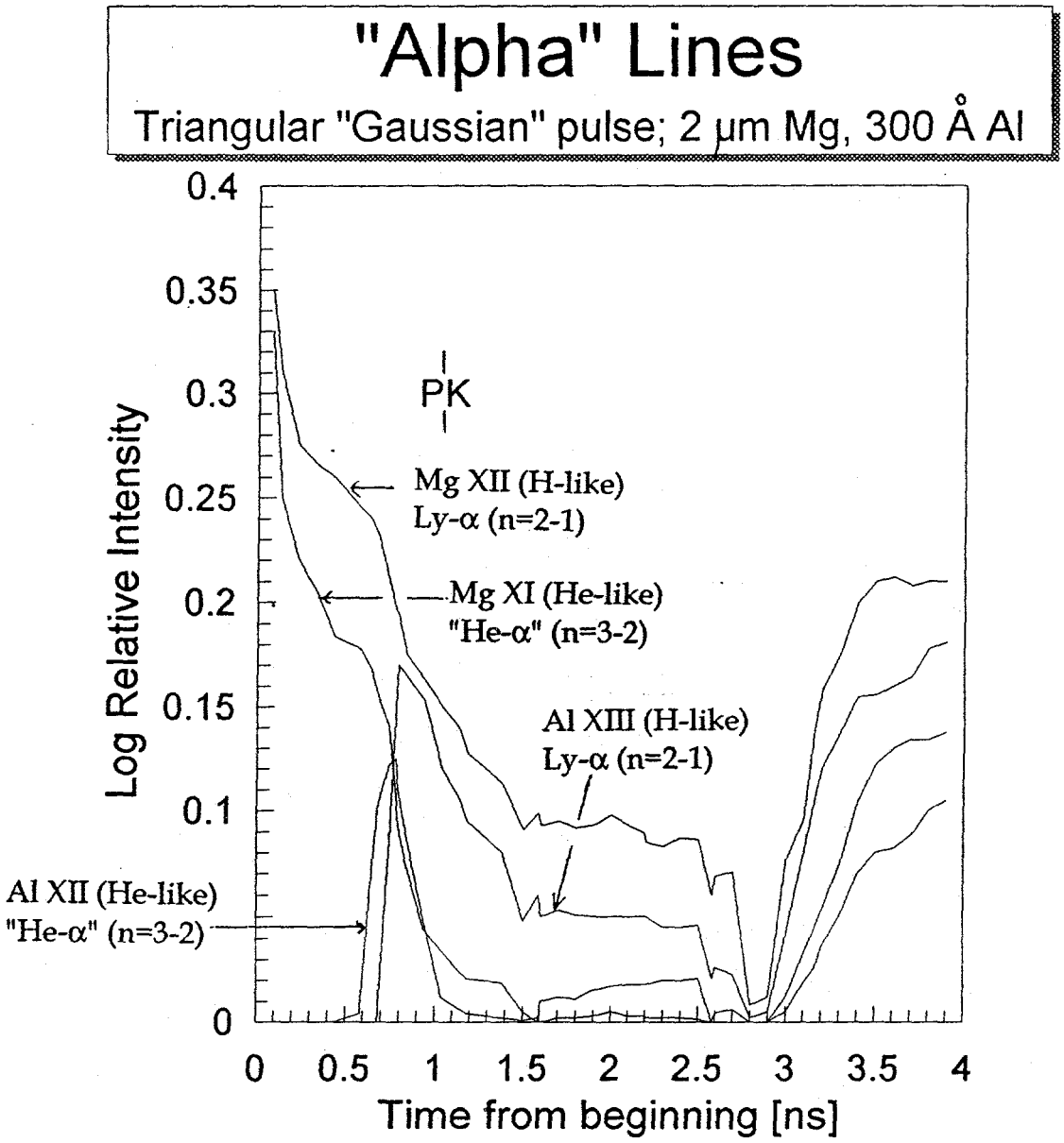

Fig. 8. Spectroscopic modeling of resonance line emission from H- and He-like ions in the Mg and Al coatings, corresponding to Fig. 7. "PK" refers to the time at which the "Gaussian" (triangular approximation) drive pulse peaks.

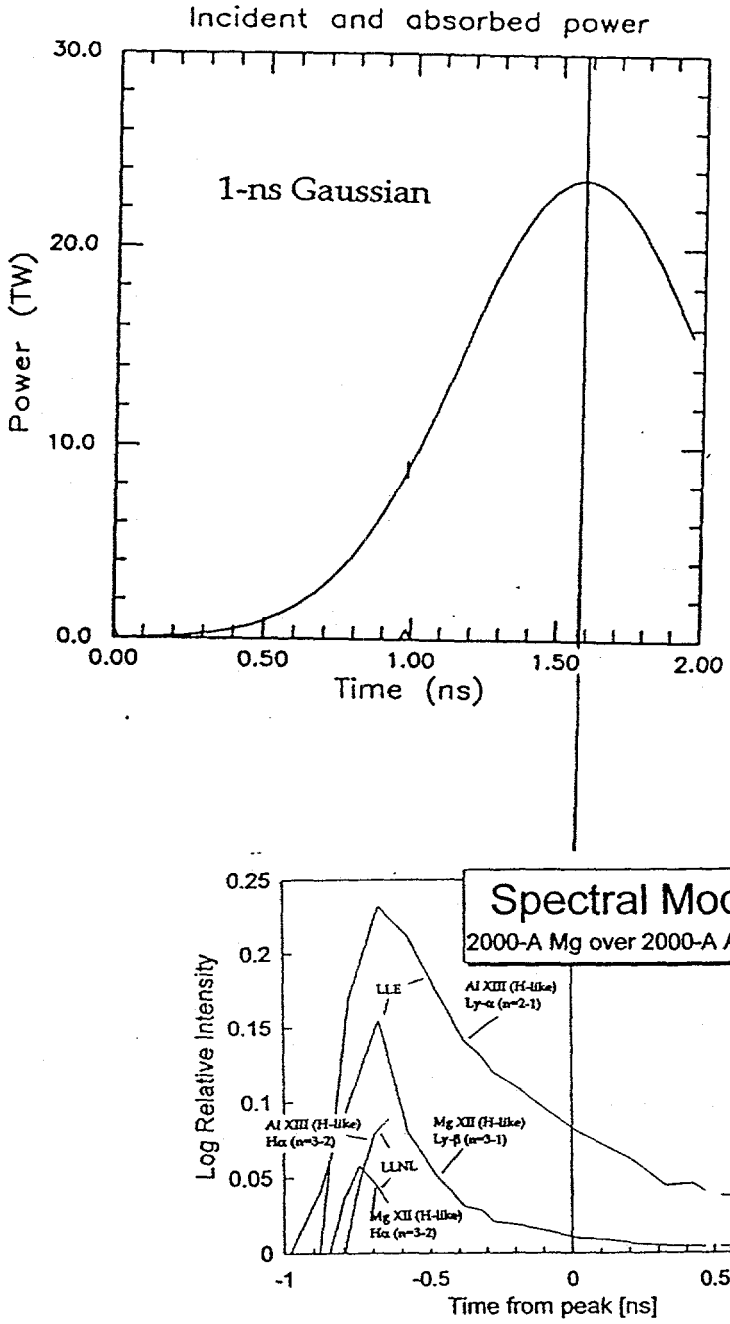

Fig. 9. Modeling (b) by LLE for an earlier case of a 2000-Å Mg coating over a 2000-Å Al coating for the Gaussian pulse shown in (a). Also shown in the lower two traces are some partial LLNL (LASNEX) modeling results for the same case, scaled down so as not to overlap the LLE results.

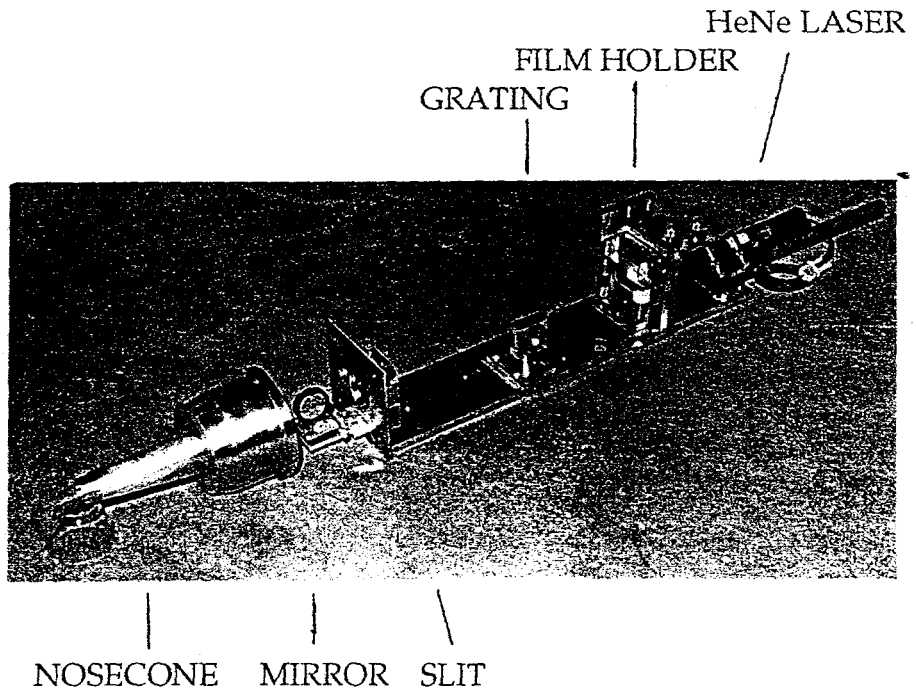

Fig. 10. Photograph of our new TIM-mounted euv spectrograph, with the nosecone and cover plates removed.